

Continuous-wave stimulated Raman scattering (cwSRS) microscopy

Zhaokai Meng · Georgi I. Petrov ·
Vladislav V. Yakovlev

Received: 24 October 2012 / Accepted: 7 March 2013 / Published online: 24 March 2013
© Springer-Verlag Berlin Heidelberg 2013

Abstract Stimulated Raman scattering (SRS) microscopy is a powerful tool for chemically sensitive non-invasive optical imaging. However, ultrafast laser sources, which are currently employed, are still expensive and require substantial maintenance to provide temporal overlap and spectral tuning. SRS imaging, which utilizes continuous-wave laser sources, has a major advantage, as it eliminates the cell damage due to exposure to the high-intensity light radiation, while substantially reducing the cost and complexity of the setup. As a proof-of-principle, we demonstrate microscopic imaging of dimethyl sulfoxide using two independent, commonly used lasers, a diode-pumped, intracavity doubled 532-nm laser and a He–Ne laser operating at 632.8-nm.

1 Introduction

Vibrational spectroscopies, such as infrared absorption [1], spontaneous Raman scattering [2, 3], and coherent anti-Stokes Raman scattering (CARS) [4–6], have been widely used as a contrast mechanism providing characteristic information about various chemical bonds. However, infrared microscopy suffers from a relatively low spatial resolution, as it relies on a long operating wavelength. Spontaneous Raman microscopy is limited to its sensitivity and, usually, is contaminated by a strong fluorescence background. CARS microscopy provides a much stronger signal and enables multiplex detection of the whole spectrum [6]. However, when extending CARS spectroscopy to

point-of-care applications, its complicated experimental setup may be problematic.

Stimulated Raman scattering (SRS) gain/loss spectroscopy originates from a nonlinear interaction between the pump (ω_p) and the Stokes (ω_s) waves in a Raman scattering medium. When the frequency difference between the pump and the Stokes waves coincides with a particular molecular vibrational frequency Ω (i.e., $\Omega = \omega_p - \omega_s$), amplification of the Stokes beam takes place. This gain is substantially reduced, if the frequencies are tuned out of the Raman resonance. Since it was first observed in 1967 [7], SRS has been used in many spectroscopic studies [8–12]. By tightly focusing both beams with a microscope objective, a strong localization of the signal to the focal volume is achieved through nonlinear optical interaction. SRS imaging has proven to non-invasively provide a chemical contrast within the sample with sub-micron spatial resolution [13, 14]. Currently, SRS microscopy is employing a variety of ultrafast laser sources [11, 12, 14–17]. However, there are several inherent problems associated with the use of ultrashort laser pulses: they are expensive, maintenance and temporal overlap might be a problem, and they are potentially harmful to living cells [13, 18]. If a continuous-wave (cw) laser is employed with an average power of 10 mW, in the focal spot of the laser beam, the light intensity as high as 10^7 W/cm² can be achieved, allowing nonlinear optical interactions to take place. Quantitatively, the cw stimulated Raman scattering (cwSRS) signal power is $\sim 2,000$ times lower than SRS using ultrafast sources (7 ps pulse width and 76 MHz repetition rate), but is still easily measurable by unsophisticated lock-in detection. Another advantage of using cw lasers is that the spectral resolution and the spectral range of SRS microscopy can be dramatically improved. For example, low-frequency Raman modes, $\Omega < 100$ cm⁻¹, such as characteristic

Z. Meng (✉) · G. I. Petrov · V. V. Yakovlev
Department of Biomedical Engineering, Texas A&M University,
College Station, TX 77843, USA
e-mail: zhaokai.meng@gmail.com; mzkmk89@tamu.edu

back-bone DNA vibrations, can be imaged for the first time in living cells [19].

In this report, we present the first application of cw lasers for microscopic SRS imaging. cwSRS microscopy may overcome difficulties introduced by their ultrafast counterparts by providing a relatively simple and inexpensive setup while keeping a low peak power density at the sample and preserving a sub-cellular spatial resolution. We note that this simple concept was first explored by Owyong and Jones [20] in 1977; however, only microscopic imaging, which is for the first time demonstrated in this report, can fully realize the great potential of this approach. A somewhat similar approach has been recently implemented in our group for CARS microscopy, when we combined a cw laser with a 10-fs Ti:sapphire oscillator for a broadband CARS imaging [21]. Quite recently, Rajapaksa and Wickramasinghe [22] used cw laser sources for tip-enhanced Raman spectroscopy-based mechanical force detection.

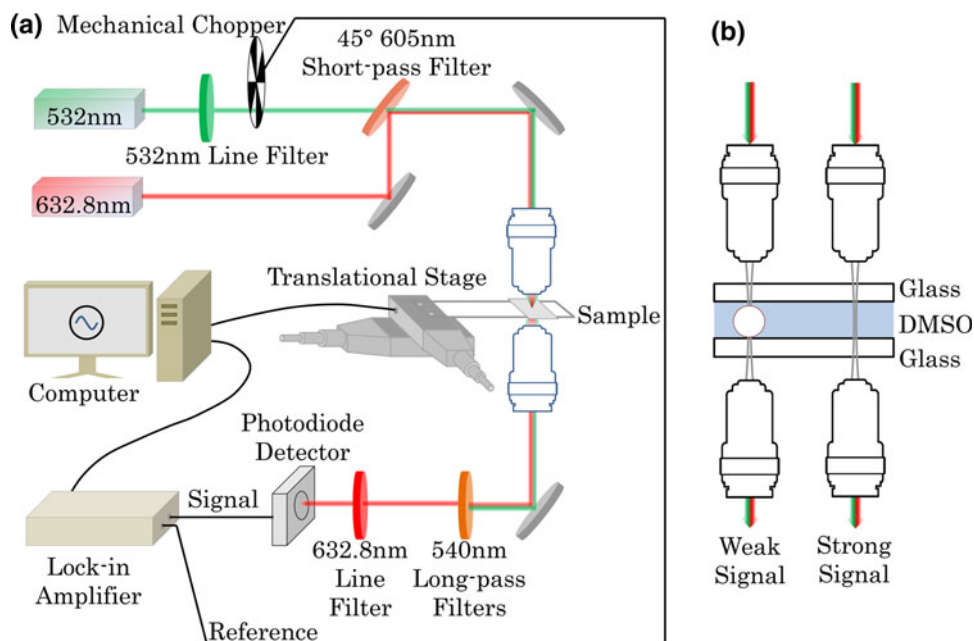
2 Methodology

The basic setup of SRS microscopy is shown in Fig. 1a. In this study, dimethyl sulfoxide (DMSO) was employed, since one of the Raman transitions can be efficiently excited using two inexpensive, commonly used and widely commercially available laser sources: a 532-nm solid state laser based on the intracavity second harmonic generation of Nd:YVO₄ fundamental wavelength (AixiZ, LLC., output power: 150 mW), and a He–Ne laser operating at 632.8-nm (output power: 15 mW). A 532-nm line filter was inserted

in the beam path of the 532-nm laser to eliminate unwanted residual spectral components. The pump and Stokes beams were combined by a 45° 605-nm short-pass filter (Semrock, Inc.). An infinity-corrected microscope objective lens (Edmund, Inc.; N.A. = 0.4) focused both beams onto the sample. Another identical objective placed in the conjugated plane was used to collect the transmitted light. Multiple Raman filters (Semrock, Inc.) were placed behind the second objective lens to block the 532-nm radiation. A 632.8-nm line filter was placed in the beam path to further clean the SRS signal. Mechanical chopper (Stanford Research Systems, Inc., model SR540) was used to modulate the beam at a frequency of about 4,000 Hz, and the modulated SRS signal was detected by an amplified photodiode (New Focus, Inc., model 2032) placed behind the filters and then transferred to a lock-in amplifier (Stanford Research Systems, Inc., model SR830a). In our experiments, the sample was placed on a computer-controlled translational stage (Micos Inc.; model SMC MT-40 2D), and the signal from the lock-in detector was analyzed as a function of the sample's position. The total average power focused on the sample was ~63 mW due to a partial attenuation by the beam delivery optics.

Figure 1b illustrates the source of the detected SRS signal. Assuming a low-gain limit, intensity of the SRS signal can be described by $I_{\text{SRS}} \propto N \times \sigma_{\text{Raman}} \times I_p \times I_s$ [23]. Here, N is the number of molecules of interest in the focal volume, σ_{Raman} is the Raman scattering cross-section for a single molecule, and I_p and I_s are intensities for the pump and the Stokes beams, respectively. To focus on the capabilities of the cwSRS microscopy, we simply chose to image the presence of DMSO in this study. Strong SRS

Fig. 1 **a** A schematic setup for cwSRS microscopy; **b** Illustration diagram of the contrast mechanism for the SRS imaging



signal manifests the presence of DMSO, while weak or no signal indicates the presence of some other substance (glass or air bubble) in the focal volume (see Fig. 1b). We confined the DMSO solution within a thin layer between two microscopic slides. The thickness of this layer was about 140 μm. The pump and the Stokes beams were focused into the layer. Additional structures made out of glass were inserted into this layer and could be imaged both using the SRS contrast mechanism and conventional optical microscopy.

Figure 2 displays the Raman spectrum of DMSO together with the measured spectra for the pump and Stokes beams. There is an overlap between the Stokes wave and DMSO’s 3,000 cm⁻¹ Raman peak, which we are exploiting here for imaging purpose.

3 Results

We first confirm that the detected signal is proportional to the incident power for both the pump and the Stokes waves and the concentration of the Raman agent. To do so, we inserted neutral density filters in either the pump or the Stokes beam path (as shown in Fig. 1), and measured the power of the signal, when two beams were focused into DMSO. Figure 3 exhibits the dependence of the SRS signal I_{SRS} on the pump (I_p), the Stokes (I_s) incident powers and

the concentration of DMSO. The figure reveals a linear dependence on both beams’ incident power, confirming the nonlinear optical nature of the detected signal. The results shown in Fig. 3 demonstrate a rather high-dynamic range of our measurements, considering a relatively low incident light power used in those experiments. We estimated that, under our present conditions, we employed less than 0.05 % peak intensity (~40 MW/cm²) of the pump used in Reference [16] (~80 GW/cm²). At the lower pump powers, the signal was limited primarily by the intrinsic noise of both lasers, which were not designed to be highly stabilized light sources. Given the recent advances of tunable diode lasers, which have their noise power level orders of magnitude lower, we expect that a much higher dynamic range of the SRS measurements can be achieved leading to much higher signal–noise ratio and lower acquisition time. However, even in the presence of such an excessive noise in the system, high-quality SRS was possible.

Figure 4 shows some of the imaging results, which were collected using cwSRS microscope setup. Figure 4a shows the SRS contrast image for a fiber end. This image was taken by scanning a 200 μm × 200 μm area with scanning speed of 100 ms per data point. The step size in each direction was 2 μm. The modulation frequency of the pump beam was 4,000 Hz. The fiber edges were clearly seen in high-dynamic range measurements, which demanded the logarithmic scale for the color plot. In order to

Fig. 2 Raman spectrum of DMSO and measured spectra for the pump and Stokes beams

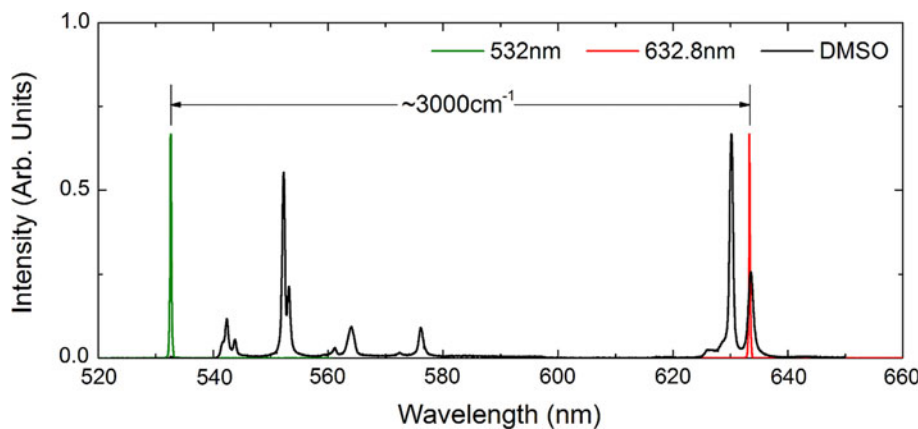
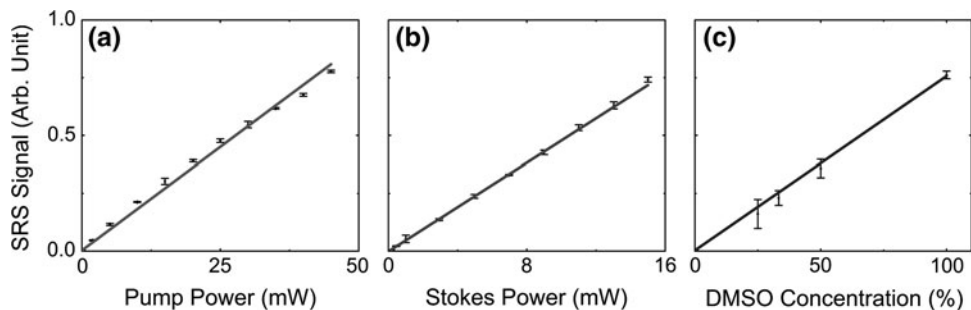


Fig. 3 SRS signal dependence on the pump (a), Stokes (b) power and DMSO concentration (c)



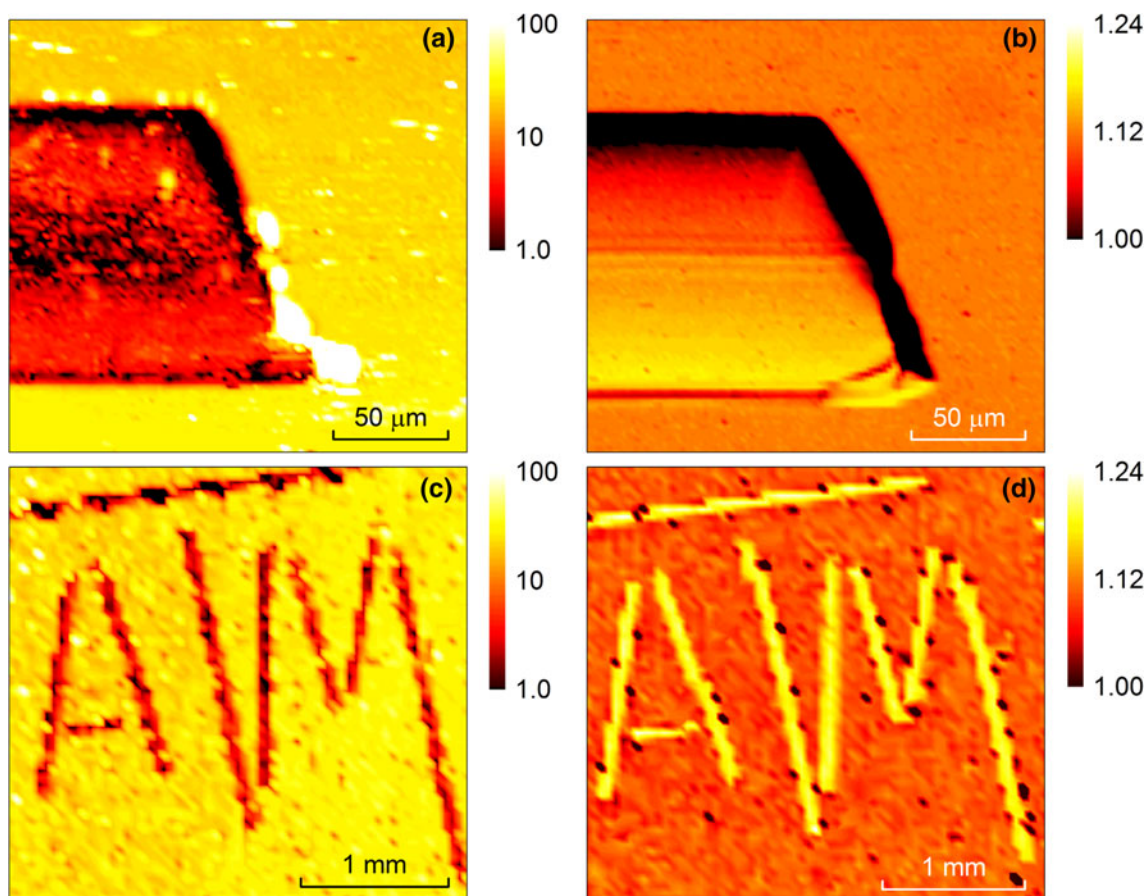


Fig. 4 **a** SRS image of a multimode optical fiber. The diameter of the fiber was $\sim 125 \mu\text{m}$. **b** The reference image of the same fiber shown in **(a)**. **c** The SRS image of a meaningful configuration of multiple fibers. Here we use an “aTm” logo of Texas A&M University. **d** The

reference image collected using light scattering contrast microscopy of the same logo shown in **(c)**. All the color images are shown in arbitrary units

distinguish contrast associated with the Raman signal (i.e. chemical specificity) from the one due to the ordinary light scattering (i.e. structural specificity), we collected a reference image as shown in Fig. 4b. To acquiring this reference scattering image, we modified the setup shown in Fig. 1a by blocking the 532-nm beam and by mechanically chopping the He–Ne laser at 4,000 Hz. All other components remained the same. Therefore, instead of SRS, linear light scattering/absorption was the main source of contrast. Since DMSO and optical fiber were both optically transparent, the intensity of the transmitted light is mainly lowered by light scattering. The image was taken by scanning the same fiber end shown in Fig. 4a. Although structural details for the fiber end also appear in this image, the dynamic range is low: besides the edge, there is only a $\sim 25\%$ contrast between the highest and the lowest signal levels. In quantitative studies, the effect of scattering/absorption should be taken into consideration, and corresponding corrections should be performed for each pixel. Figure 4c, d shows SRS and reference images for a meaningful composition made by multiple fibers. Here we

use an “aTm” logo for Texas A&M University. The images were derived by scanning a $3.1 \text{ mm} \times 3.1 \text{ mm}$ area. In order to get a fast scan we chose a step size as large as $50 \mu\text{m}$ for both images in both directions. Comparing with the reference image, the SRS image again shows a higher contrast and therefore induces a greater dynamic range.

4 Discussion

Microscopic optical imaging with a contrast provided by vibrational spectroscopy is important for biomedical research and material sciences. In this paper, we have demonstrated that cwSRS microscopy is a valuable addition to the family of SRS imaging instruments. It allows high spectral resolution and low-frequency Raman measurements. Recent advances of tunable diode lasers may help overcoming the first drawback, as well as enabling ultrahigh spectral resolution and high short- and long-term stability. The high spectral resolution of cwSRS microscopy enables imaging low-frequency Raman modes, such

as the DNA double helix vibrational modes, and various low-frequency modes in protein molecules [19, 24, 25]. However, under current setup, cwSRS setup is unable to make multiplex Raman/CARS spectrum detections, such as spontaneous Raman scattering or multiplex coherent anti-Stokes Raman scattering (MCARS) [6, 26]. Comparing with ultrafast laser sources, the relatively narrower tunable range (<100 nm, or $<1,000$ cm^{-1}) for cw lasers is another drawback for cwSRS. Multiple or tunable cw sources covering different spectral ranges can be utilized, and those experiments are currently underway in our laboratory.

Comparing with previous implementations of SRS microscopies, a relatively low peak power of cwSRS is another advantage. Previous studies indicate that the probability of cell damage is inversely correlated with the laser pulse duration [18, 27, 28]. The use of cw radiation fully excludes this type of damage, leaving the average power effect as the only limiting parameter. Since SRS gain/loss spectroscopy is, essentially, the heterodyne detection of a weak Raman signal, the signal to noise ratio, as it was demonstrated by Eesley et al. [29] will be determined by the total number of generated Raman photons, i.e. by the average incident average power. We can scale down the acquisition time in our experiments, by noting that the strength of the Raman line we were using as a molecular marker is comparable to the strength of CH_2 vibration in lipids. The average power can be increased by a factor of 10 without harming living cell, and the signal-to-noise can be reduced to the level of 3–4, while still providing good quality images. Provided the proper modulation and detection, this leads to a dwell time as little as 1 μs per pixel, which is sufficient for video rate imaging.

5 Summary

In summary, we have demonstrated that cwSRS microscopy is a possible alternative of the pulsed laser-based SRS microscopies. cwSRS provides high-dynamic range, yet low cost and relatively simple approach for potential biomedical imaging applications. Comparing with ultrafast laser sources, cwSRS is capable to improve the spectral resolvability, while reduce the peak power and consequently the photodamage rate of the sample. While our current cwSRS system is able to capture high-dynamic range images, several follow-up studies may be required either to further characterize cwSRS microscopy or to improve this imaging modality. The same concept can also be extended for stimulated Raman photoacoustic imaging [21, 30].

Acknowledgments This work was partially supported by the start-up funds available through Texas A&M University. Authors also acknowledge the support of the NIH (Grant #R21EB011703) and the NSF (ECS Grant #0925950, DBI Grant #0964225, and CBET Grant #1066562).

References

1. G. Barrow, *Molecular Spectroscopy* (McGraw-Hill, New York, 1962)
2. C. Raman, K. Krishnan, *Nature* **121**, 711 (1928)
3. G. Puppels, F. de Mul, C. Otto, J. Greve, M. Robert-Nicoud, D. Arndt-Jovin, T. Jovin, *Nature* **347**(6290), 301 (1990)
4. M.D. Duncan, J. Reintjes, T.J. Manuccia, *Opt. Lett.* **7**(8), 350 (1982)
5. A. Zumbusch, G. Holtom, X. Xie, *Phys. Rev. Lett.* **82**(20), 4142 (1999)
6. C.H. Camp, S. Yegnanarayanan, A.A. Eftekhar, H. Sridhar, A. Adibi, *Opt. Express* **17**(25), 22879 (2009)
7. N. Bloembergen, *Am. J. Phys.* **35**(11), 989 (1967)
8. A. Owyong, *Opt. Commun.* **22**(3), 323 (1977)
9. B. Levine, C. Shank, J. Heritage, *IEEE J. Quantum Electron.* **15**(12), 1418 (1979)
10. P. Kukura, D. McCamant, S. Yoon, D. Wandschneider, R. Mathies, *Science* **310**(5750), 1006 (2005)
11. E. Ploetz, S. Laimgruber, S. Berner, W. Zinth, P. Gilch, *Appl. Phys. B Lasers Optics* **87**(3), 389 (2007)
12. P. Nandakumar, A. Kovalev, A. Volkmer, *New J. Phys.* **11**(3), 033026 (2009)
13. J. Squirrell, D. Wokosin, J. White, B. Bavister, *Nat. Biotech.* **17**(8), 763–767 (1999)
14. B. Saar, C. Freudiger, J. Reichman, C. Stanley, G. Holtom, X. Xie, *Science* **330**(6009), 1368 (2010)
15. P. Kukura, D. McCamant, R. Mathies, *Annu. Rev. Phys. Chem.* **58**, 461 (2007)
16. C. Freudiger, W. Min, B. Saar, S. Lu, G. Holtom, C. He, J. Tsai, J. Kang, X. Xie, *Science* **322**(5909), 1857 (2008)
17. Y. Ozeki, F. Dake, S. I. Kajiyama, K. Fukui, K. Itoh, *Opt. Express* **17**(5), 3651–3658 (2009)
18. V.V. Yakovlev, *J. Raman Spectrosc.* **34**(12), 957 (2003)
19. H. Urabe, H. Hayashi, Y. Tominaga, Y. Nishimura, K. Kubota, M. Tsuboi, *J. Chem. Phys.* **82**(1), 531 (1985)
20. A. Owyong, E.D. Jones, *Opt. Lett.* **1**(5), 152 (1977)
21. V.V. Yakovlev, H.F. Zhang, G.D. Noojin, M.L. Denton, R.J. Thomas, M.O. Scully, *Proc. Natl. Acad. Sci. USA* **107**(47), 20335 (2010)
22. I. Rajapaksa, H.K. Wickramasinghe, *Appl. Phys. Lett.* **99**(16), 161103 (2011)
23. Y.R. Shen, *The principles of nonlinear optics* (Wiley, New York, 1984)
24. H. Urabe, Y. Tominaga, K. Kubota, *J. Chem. Phys.* **78**, 3 (1983)
25. K. Chou, *Biochem. J.* **215**(3), 465–469 (1983)
26. J. Camp, S. Yegnanarayanan, A. Eftekhar, A. Adibi, *Opt. Lett.* **36**(12), 2309–2311 (2011)
27. A. Hopt, E. Neher, *Biophys. J.* **80**(4), 2029–2036 (2001)
28. Y. Fu, H. Wang, R. Shi, J. Cheng, *Opt. Express* **14**(9), 3942–3951 (2006)
29. G. Eesley, M. Levenson, W. Tolles, *IEEE J. Quantum Electron.* **14**(1), 45 (1978)
30. V. Yakovlev, G. Petrov, G. Noojin, C. Harbert, M. Denton, R. Thomas, *J. Biophotonics* **3**(10–11), 653 (2010)